J Mater Sci: Mater Med (2008) 19:311–318
DOI 10.1007/s10856-006-0020-2

Synthesis and characterization of bioresorbable in situ crosslinkable ultra low molecular weight poly(lactide) macromer

Esmaiel Jabbari · Xuezhong He

Received: 19 March 2006 / Accepted: 19 October 2006 / Published online: 28 June 2007

Abstract Reactive low molecular weight poly(L-latide) (PLA) is required to produce in situ hardened scaffolds with fast rate of crosslinking, high crosslink density, and adequate mechanical strength. The objective of this work was to synthesize unsaturated ultra low moelcular weight PLA (ULMW PLA) as an injectable in situ crosslinkable macromer for biomedical applications. Low molecular weight PLA was synthesized by ring-opening polymerization of L-lactide (LA) using diethylene glycol (DEG) as the initiator. The molar ratio of the LA to DEG ranged from 5 to 20. Non-solvents methanol, ether, and hexane were used for purification and fractionation. The PLA samples that were precipitated in methanol and ether had narrow distributions (PDI = 1.2) and resulted in a powder with M_n of 4.8 and a wax with M_n of 3.6 kDa, respectively. The PLA sample in which the supernatant from ether was re-precipitated in hexane produced a viscous ULMW PLA with M_n and PDI of 1.2 kDa and 1.2, respectively. The ULMW PLA was reacted with fumaryl chloride to produce unsaturated in situ crosslinkable poly(lactide fumarate) (PLAF) macromer. Porous scaffolds were produced after injection and in situ crosslinking of the PLAF macromer with NVP crosslinker in the presence of a porogen. New bone was formed in the scaffold when it was implanted in nude mice which demonstrated that the scaffold was osteoconductive. PLAF is potentially useful as a reactive macromer in fabrication of bioresorbable injectable in situ crosslinkable scaffolds for tissue regeneration.

E. Jabbari · X. He
Biomimetic Materials and Tissue Engineering Laboratories, Department of Chemical Engineering, University of South Carolina, Columbia, SC 29208, USA

E. Jabbari (✉)
Department of Chemical Engineering, Swearingen Engineering Center, Rm 2C11, University of South Carolina, Columbia, SC 29208, USA
e-mail: jabbari@engr.sc.edu

Introduction

PLA is the most widely used resorbable polymer in the biomedical field [1]. PLA and its copolymers with poly(glycolic acid) (PGA) are being used in a wide range of clinical applications which include resorbable sutures [2], resorbable sheets for temporary wound support [3], dialysis media [4], intradermal implants for facial augmentation [5], drug delivery systems [6] and orthopaedic fixation devices [7, 8]. PLA is also evaluated as a biomaterial in fabrication of tissue engineering scaffolds [9–12], particularly for bone tissue engineering [13–15], because its degradation product, lactic acid, is resorbed through the metabolic pathways [16]. Furthermore, the flexibility in its design allows the synthesis of a wide range of polymers with varying mechanical, biologic and degradation properties to suit various applications [17]. PLA can also be modified with biomiemtic funcional groups to support cell migration, atttachment, differentiation, and proliferation and to make the scaffold conductive to tissue in-growth [18].

One approach to tissue regeneration is the use of prefabricated scaffolds for cell transplantation [19, 20]. The other approach involves the use of injectable and in situ crosslinkable biodegradable polymers [21, 22]. Rigid scaffolds must be implanted surgically, while ductile scaffolds can be injected, reducing the invasiveness of the implantation procedure. Moreover, injectable scaffolds are

more suitable for treating irregularly shaped defects and provide good bonding to the surrounding tissues. Degradable macromers such as poly(anhydrides) [23], poly(propylene fumarate) [24], and polyurethanes [25] have recently been developed to harden in situ when injected into a cavity by minimally invasive arthroscopic procedures. However, these macromers are not FDA approved and their degradation profile can not be tailored to a particular application.

PLA is a biodegradable thermoplastic polymer which is FDA approved for a number of clinical applications [2–8], but PLA can not be crosslinked in situ, requiring an invasive surgical procedure for implantation. Furthermore, high temperature or dissolution in toxic organic solvents is required to soften the PLA for injection which is not compatible with cells and proteins [26–28]. More importantly, commercially available PLA, when functionalized with acrylate, methacrylate, or fumarate groups, has a low rate of crosslinking due to low density of reactive groups and slow diffusivity of the polymer chains [29]. Therefore, for minimally invasive surgical procedures, ultra low molecular weight (ULMW) PLA is required to produce in situ hardened scaffolds with a relatively fast rate of crosslinking, high density of crosslinks, and adequate mechanical strength. In commercially available PLA, after synthesis, the polymer is precipitaed in methanol to remove the unreacted monomer, initiator and catalyst [30]. However, precipitation of the product in methanol removes the low molecular weight PLA fractions [31].

The development of injectable PLA macromers requires the synthesis of ULMW PLA with relatively narrow molecular weight distribution. The objective of this work was to synthesize unsaturated ULMW PLA as an injectable in situ crosslinkable macromer for fabrication of tissue engineering scaffolds. PLA can be synthesized by condensation polymerization of lactic acid [32] or ring-opening polymerization of L-lactide monomer [33]. The ring-opening polymerization of L-lactide was selected in this work because the living character of the initaion step results in the formation of relatively narrow distribution polymer [34].

Experimental

Materials

L-lactide monomer (LA; >99.5% purity by GC) was purchased from Ortec, Inc. (Easley, SC). Di(ethylene glycol) (DEG; >99% purity), tin(II) 2-ethylhexanoate (TEH), triethylamine (TEA), anhydrous ethyl acetate, and fumaryl chloride (FuCl) were purchased from Aldrich (Milwaukee, WI). FuCl was purified by distillation at 161 °C. 1-vinyl-2-pyrrolidinone (NVP) was purchased from Aldrich and used as recieved. Dichloromethane (DCM; Fisher Chemicals, Pittsburg, PA) was dried by distillation over calcium hydride (Aldrich). All other solvents (Fisher) were used as recieved.

Polymerization

ULMW PLA synthesis: PLA was synthesized by ring-opening polymerization of LA monomer using DEG and TEH as the bifunctional initiator and polymerization catalyst, respectively [30]. The molar ratio of DEG to TEH was 5:1. The molar ratio of LA to DEG was varied from 5 to 20 to produce PLA with number average molecular weights ($\overline{M_n}$) ranging from 1 to 5 kDa. In a typical procedure, 18 g LA (0.125 mol) was added to a three-neck reaction flask, equipped with a mechanical overhead stirrer under nitrogen atmosphere. The reaction vessel was submerged in an oil bath and gradually heated to 110–120 °C under a steady flow of nitrogen gas to melt the monomer. After complete melting, 1.66 g DEG (0.0157 mol) and 1.0 ml TEH were added to the reaction. The polymerization reaction was allowed to proceed for 4 h at 120 °C and continued for an additional 20 h at 140 °C. After the reaction, the unreacted LA and DEG were removed under vaccum (<1 mm Hg) at 140 °C for at least 6 h. The reaction product was dissolved in DCM and precipited in ice cold methanol, ether, or hexane to fractionate the PLA product. The solvent was decanted and the polymer was vacuum dried (<5 mmHg) to remove any residual solvent. The final purified PLA was stored at –20 °C.

Poly(lactide fumarate) synthesis: The PLAF macromer was synthesized by condensation polymerization of ULMW PLA with FuCl [35]. TEA was used as the catalyst for the reaction. The molar ratio of FuCl:PLA and TEA:-PLA was 0.98:1.0 and 2:1, respectively. In a typical reaction, 20 g of ULMW PLA was dissolved in DCM under dry nitrogen atmosphere in a three-neck reaction flask. The reaction vessel was placed in an ice bath to limit the temperature increase caused by the exothermic reaction. Next, FuCl (0.6 ml) and TEA (1.6 ml), each dissolved in DCM, were added dropwise to the reaction with stirring. The reaction was continued for 12 h under ambient conditions. After completion of the reaction, solvent was removed by rotovaporation, residue was dissolved in anhydrous ethyl acetate, and the by-product triethylamine hydrochloride salt was removed by filtration. Ethyl acetate was removed by vacuum distillation, the macromer was redissolved in DCM and precipitated twice in ice cold ethyl ether. It was dried in vacuum (less than 5 mmHg) at ambient temperature and stored at –20 °C.

PLAF crosslinking and scaffold fabrication: PLAF was mixed with 30% NVP (based on the PLAF weight). Hydroxyapatite nano-particles (Berkeley Advanced Biomaterials, Berkeley, CA), 10% based on the weight of PLAF, was added to improve compressive strength of the scaffold [36]. 4.0 g NaCl crystals per gram PLAF was added to the polymerizing mixture as the porogen, corresponding to 65% by volume porosity. 50 µl per gram PLAF benzoyl peroxide (BPO) solution (50 mg of BPO in 0.25 ml of NVP) as the initiator and 40 µl per gram PLAF dimethyl toluidine (DMT) solution (40 µl of DMT in 0.96 ml of DCM) as the accelerator were added to the mixture. The polymerizing mixture was transferred to an 8×3 mm cylindrical Teflon mold and pressed to maximize packing. The mold was placed in an oven at 37 °C for 15 min to facilitate crosslinking. After crosslinking, the scaffolds were soaked in deionized water for 1 h to leach out most of the porogen. The pore morphology was studied by scanning electron microscopy.

Characterization

The chemical structure of the synthesized PLA and PLAF was characterized by a Variam Mercury-300 ^{1}H-NMR (Varian, Palo Alto, CA) at ambient conditions. Pulse angle, pulse width, recycle time, aquisition time, resolution, and number of scans were 90°, 4.8 µs, 1 s, 3 s, 0.17 Hz, and 16, respectively. The polymer sample was dissolved in deuterated chloroform (Aldrich, 99.8 atom % deuterated) at a concentration of 50 mg/ml and 1% v/v trimethylsilane (TMS; Aldrich) was used as the internal standard.

The molecular weight distribution of the synthesized PLA and PLAF was measured by gel permeation chromatography (GPC) [37]. Measurements were carried out with a Waters 717 Plus Autosampler GPC system (Waters, Milford, MA) connected to a model 616 HPLC pump, model 600S controller, and a model 410 refractive index detector. The columns consisted of a styragel HT guard column (7.8×300 mm, Waters) in series with a styragel HR 4E column (7.8×300 mm, Waters) heated to 37 °C in a column heater. The GPC unit was operated using a multisystem millennium operating system and the Empower software was used for data analysis and determination of the number ($\overline{M_n}$) and weight ($\overline{M_w}$) average molecular weights and polydispersity index (PI). The sample (20 µl), with a concentration of 10 mg/ml in tetrahydrofuran (THF; Aldrich), was eluted at a flow rate of 1 ml/min. Twelve monodisperse polystyrene standards (Waters) with peak molecular weights (M_p) ranging from 0.58 to 143.4 kDa and polydispersities of less than 1.1 were used to construct the calibration curve.

The viscosity of the PLAF polymerizing mixture was measured with an AR-2000 Rheometer (TA Instruments, New Castle, DE) using parallel plate geometry. The upper plate was a 20 mm diameter disk. The upper plate was lowered to a gap of 800 µm, a sinusoidal shear strain was applied to the sample, and the required torque was measured as a function of temperature. The experiments were conducted with a peak sinusoidal shear strain of 0.5% (linear viscoelastic region).

A Perkin Elmer differential scanning calorimeter DSC-7 was used to characterize the melting transition of the monomer, synthesized PLA and PLAF. DSC measures the differential amount of heat absorbed by the sample as the sample is heated at a rate of 5 °C/min. A Perkin Elmer thermogravimetric analyzer TGA-7 was used to measure the stability of the PLA and PLAF with increasing temperature. TGA measures the change in the weight of a polymer sample as it is heated from ambient to well above the degradation temperature of the polymer. The sample was heated to 100 °C, allowed to equilibrate for 15 min to remove moisture, and heated to 500 °C at a rate of 10°C/min. The TGA and DSC experiments were carried out under a flow of helium gas (60 ml/min).

The pore morphology of the scaffolds was studied with an environmental scanning electron microscope (ESEM) FEI XL30 equipped with an electron backscattered detector. The scaffold was attached to the SEM stub with a double-sided tape and imaged at an accelerating voltage of 30 kV.

In vivo implantation

Osteoconductivity of the scaffolds was evaluated in vivo by subcutaneous implantation in nude mice (Harlan, USA) [38]. Protocols for all operative procedures were approved by the Institutional Animal Care and Use Committee. Osteoblasts were isolated from 1–3 mm strips of immature bone taken from the femur and tibia of fetal calves. The bone strips were carefully removed of periosteum and cartilage, and dispersed enzymatically using 0.5 mg/ml collagenase. Cells were dissociated from bone fragments by vortexing and removed by sedimentation. Cells were collected from the supernatant by centrifugation. The resulting cell suspension was seeded at a density of 1×10^4 cell/cm^2 and cultured in complete media (DMEM with 10% FBS, 10 ml of 1% (v/v) antibiotic and antimycotic agents, 10^{-3} M β-glycerol phosphate, and 50 mg/l L-ascorbic acid). After reaching confluency, cells were enzymatically lifted and loaded into porous scaffolds. PLAF scaffolds were sterilized in excess 70% ethanol and rinsed in phosphate buffer saline (PBS) before cell seeding. Loaded disks (8×2 mm; 1.5×10^6 cells/implant) were implanted subcutaneously in the back of nude mice. The animals were anesthetized with 80 and 5 mg/kg ketamine and xylazine, respectively. Six weeks after implantation,

the animals were sacrificed and samples were removed. Samples were demineralized, dehydrated in sequential ethanol solution, embedded in paraffin, sectioned into 5 μm thick sections. Sections were stained with Hematoxylin and Eosin (H&E) for histological examination.

Results and discussion

DEG has a low toxicity and boiling point of less than 100 °C at 1 mmHg [39]. Therefore, the unreacted monomer and DEG (vaporization temperatures of well below 140 °C) were removed from the reaction product by the application of vacuum of 1 mmHg at 140 °C, as shown in the GPC chromatograms in Fig. 1.

The choice of the non-solvent for PLA precipitaion depended on the LA:DEG ratio. When methanol was used as the precipitation solvent, the monomer and low molecular weight fractions (<4 kDa), which are soluble in methanol, were removed from the precipitate. Furthermore, as the ratio of the LA:DEG was reduced to below 20, only a small fraction of the PLA precipitated in methanol. Therefore, methanol was not suitable as a non-solvent for precipitation and isolation of ULMW PLA, even though it effectively removed the unreacted monomer. Before applying vacuum, when the synthesized PLA was precipitaed in ether, the precipiate had a lower molecular weight ($\overline{M_n}$ = 3.6 kDa, see Table 1) compared to that of methanol ($\overline{M_n}$ = 4.8 kDa), but the LA monomer, being insoluble in ether, precipitated with the polymer. This is shown in Fig. 1 (chromatogram b), where a peak coresponding to the elution of LA can be observed. When the reaction product was precipiated in ether after the application of vacuum (<1 mmHg at 140 °C for 6 h), the monomer peak was absent in the precipitate (Fig. 1, chromatogram c). A relatively larger fraction of the polymer precipitated when hexane was used as the non-solvent, and the molecular weight of the precipitate was significantly lower ($\overline{M_n}$ = 2.3 kDa) than that of the ether and methanol but the polydispersity index (PDI) was higher (1.6 for hexane compared to 1.3 and 1.2 for ether and methanol, respectively). These results demonstrate that low ratios of LA:-DEG, vacuum separation of the unreacted monomer and initiator, and precipitation of the reaction product in ether or hexane can be used to synthesize and purify ULMW PLA.

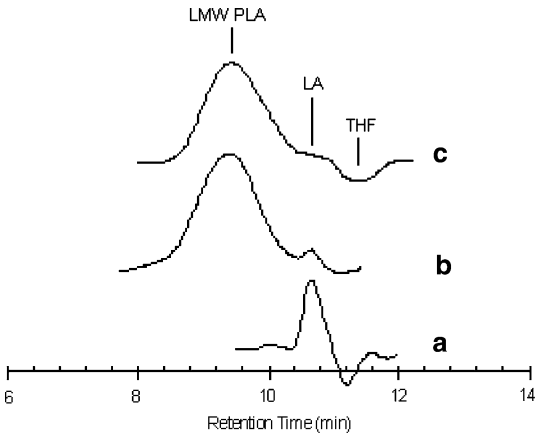

Fig. 1 GPC chromatogram of LA (**a**), ULMW PLA product without (**b**) and with (**c**) the application of vacuum after the polymerization reaction. The PLA was synthesized with LA:DEG ratio of 10

Table 1 Effect of LA:DEG ratio and precipitation solvent on molecular weight of the synthesized ULMW PLA

LA:DEG ratio	Precipitation solvent	M_n	M_w	PI
20	Methanol	6,830	9,070	1.3
10	Methanol	4,850	5,960	1.2
10	Ether	3,560	4,100	1.3
10	Hexane	2,330	2,900	1.6
5	Hexane	1,030	2,080	2.0

^{1}H-NMR and FTIR were used to characterize the chemical structure of the PLA and PLAF. The ^{1}H-NMR spectrum of the synthesized PLA (LA:DEG = 10) after precipitation in ether and that of PLAF (the insert) are shown in Fig. 2. A singlet chemical shift with peak position at 1.6 ppm, two triplets with peak positions at 3.6 and 4.2 ppm, and a quartet with peak location at 5.1 ppm were observed in the NMR spectrum of the PLA. The singlet chemical shift with peak position at 1.6 ppm was attributed to the hydrogens of the methyl group (–CH_3) of lactide monomer [40]. The triplet chemical shifts centered at 3.6 and 4.2 ppm were due to the hydrogens of the methylene groups on the initiator, DEG, attached to the ether group (–CH_2–O–CH_2–) and to the ester group of the PLA (–CH_2–OOC–), respectively [40]. The quartet chemical shift with peak position at 5.1 ppm was due to the hydrogens attached to the methine group of the PLA. The ratio of the chemical shifts in the NMR specttrum at 3.6 ppm (due to the methylene hydrogens attached to the ether group (–CH_2–O–CH_2–) of the initiator) and 5.1 ppm (due to the methine hydrogen of the lactide repeat unit) was directly related to the degree of polymerization and $\overline{M_n}$ of the polymer. The PLA with $\overline{M_n}$ of 3.3 kDa, based on GPC data, resulted in the NMR monomer to initiator peak ratio of 42, corresponding to $\overline{M_n}$ of 3.1 kDa. Therefore, the $\overline{M_n}$ values determined from the NMR peak ratio were consistent with the $\overline{M_n}$ values obtained from the GPC data.

The ^{1}H-NMR spectrum of the PLAF is shown as an insert in Fig. 2. The additional singlet shifts at 6.90 and 6.95 ppm were attributed to the methine hydrogens of the

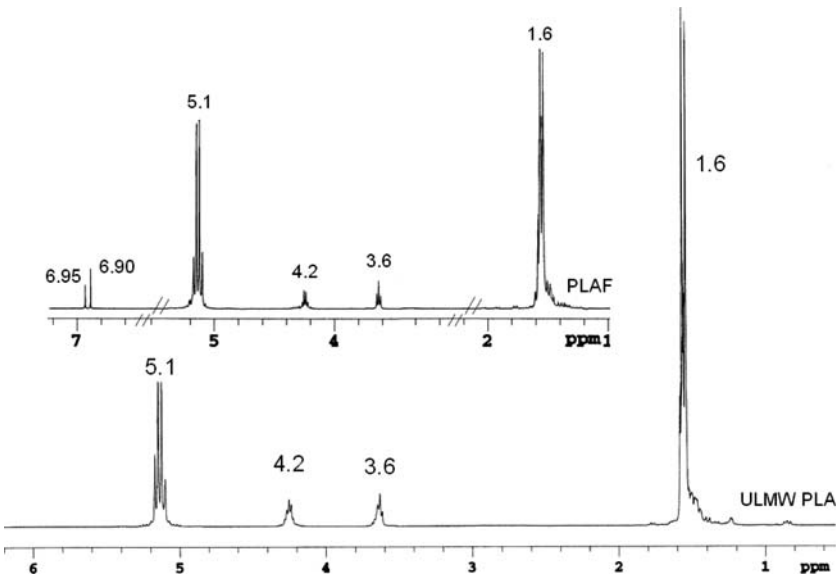

Fig. 2 ^{1}H-NMR spectrum of the ULMW PLA and PLAF (insert)

fumarate in the middle of the chain (–OOC–CH=CH–COO–) and at the chain ends (–OOC–CH=CH–COOH), respectively. The presence of peaks at 6.90 and 6.95 ppm in the NMR spectrum attributable to the hydrogens of the fumarate groups, and the presence of a band due to the ester carbonyl stretching vibration centered at 1,725 cm^{-1} in the FTIR spectra (data not shown), confirmed the incorporation of fumarate monomers in the PLAF macromer. The PLAF macromer with PLA molecular weight of 1.2 kD (PI 1.2) had $\overline{M_n}$ and PDI of 4.1 kD and 1.5, respectively, as determined by GPC.

Table 1 shows the effect of LA:DEG ratio and precipitation solvent on the molecular weight distribution of PLA. The PLA with LA:DEG ratio of 20 had a significant precipitate fraction in methanol (>75%) with $\overline{M_n}$ and PDI of 6.8 kDa and 1.3, respectively. The PLA with LA:DEG ratio of 10 had a low precipitate fraction in methanol (<20%) and greater than 60 and 90% precipitate in ether and hexane respectively. The PLA with LA:DEG ratio of 5 had a significant precipitate fraction in hexane with $\overline{M_n}$ of 1.0 kDa and a relatively large PDI of 2. The PLA with LA:DEG ratio of 10 had a $\overline{M_n}$ of 4,850, 3,560, 2,330 Da and PDI of 1.2, 1.3, 1.6 when precipitated in methanol, ether, and hexane, respectively. Direct precipitation in hexane resulted in a PLA polymer with a relatively wide distribution compared to that of methanol or ether.

To produce narrow distribution ULMW PLA, double precipitation in two non-solvents was used, as shown in Table 2. The synthesized PLA was precipitated in the first non-solvent (methanol or ether) and the supernatant was re-precipitated in the second non-solvent (hexane). When methanol was used as the first non-solvent, the $\overline{M_n}$ and PDI of the precipitate was 4.8 kDa and 1.2 and that of the second precipitate in hexane was 2.3 kDa and 1.5. When ether was used as the first non-solvent, the $\overline{M_n}$ and PDI of the precipitate was 3.5 kDa and 1.2 and that of the second precipitate in hexane was 1.3 kDa and 1.3, respectively. A non-solvent mixture ranging from 100:0 to 80:20 ether:methanol ratio was used as the non-solvent in the first precipitation and the supernatant was re-precipitated in hexane. The molecular weight distribution results are presented in Table 3. A slight decrease in molecular weight (<3%) was obtained when 0–20% methanol was added to

Table 2 Effect of double precipitation on molecular weight distribution of the ULMW PLA

Double precipitation	Precipitation solvent	M_n	M_w	PI
1st Precip.	Methanol	4,850	5,960	1.2
2nd Precip.	Hexane	2,320	3,580	1.5
1st Precip.	Ether	3,560	4,100	1.2
2nd Precip.	Hexane	1,290	1,700	1.3

Table 3 Effect of ether:methanol solvent ratio in the first precipitation on molecular weight distribution of the ULMW PLA

Ether:Methanol ratio in 1st precipitation	Double precipitation	M_n	M_w	PI
100:0	1st Precip.	3,560	4,100	1.2
	2nd Precip.	1,290	1,700	1.3
95:5	1st Precip.	3,490	4,000	1.2
	2nd Precip.	1,230	1,630	1.3
85:15	1st Precip.	3,440	3,960	1.2
	2nd Precip.	1,270	1,660	1.3
80:20	1st Precip.	3,330	3,860	1.2
	2nd Precip.	1,220	1,620	1.3

the ether in the first precipitation, while the polydispersity remained unchnaged.

The GPC chromatograms of the synthesized PLA, precipitated in different non-solvents, are shown in Fig. 3. The PLA sample precipitated in methanol and ether was relatively monodisperse (PDI = 1.2) with $\overline{M_n}$ of 4.8 and 3.6 kDa, respectively (chromatograms b and c). The PLA sample precipitated directly in hexane was relatively polydisperse (PDI = 1.6) with $\overline{M_n}$ of 2.3 kDa (chromatogram d). The PLA sample in which the supernatant from ether was re-precipitated in hexane had a narrow distribution with $\overline{M_n}$ of 1.2 kDa (chromatogram e). The PLA sample with $\overline{M_n}$ of 1.2, 3.5, and 4.8 kDa and equal polydipersity indices of 1.2 were viscous liquid, wax, and powder at ambient conditions, respectively. The GPC chromatograms of the ULMW PLA and the corresponding PLAF are shown in Fig. 4. The PLA which was precipitated in ether and then reprecipitaed in hexane had $\overline{M_n}$ and PDI of 1.2 kDa and 1.2, respectively. The PLAF had a wider molecular weight distribution (due to the step-growth nature of the reaction between PLA and FuCl) with PDI of 1.5 and Mn of 4.1 kDa. There was, on average, 3.1 reactive fumarate groups per PLAF chain.

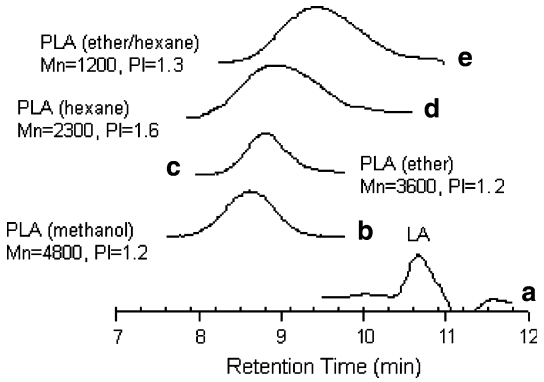

Fig. 3 GPC chromatogram of LA (**a**), PLA product by precipitation in methanol (**b**), in ether (**c**), in hexane (**d**), and PLA produced by precipitating the supernatant from ether precipitation in hexane (**e**). The PLA was synthesized with LA:DEG ratio of 10

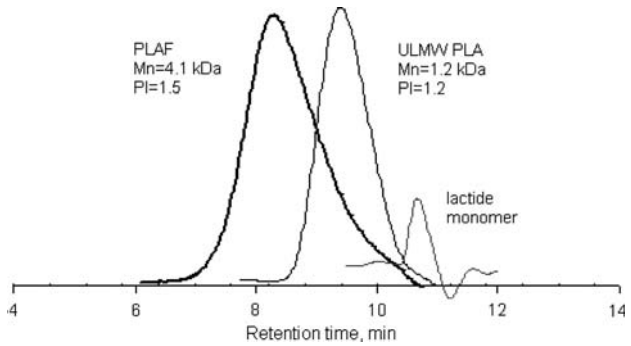

Fig. 4 GPC chromatogram of LA, ULMW PLA, and the corresponding PLAF. The PLA was synthesized with LA:DEG ratio of 10

The DSC and TGA of the LA, ULMW PLA (M_n = 1.2 kDa and PDI = 1.2), and PLAF (M_n = 4.1 kDa and PDI = 1.5) are shown in Figs. 5 and 6, respectively. The DSC thermogram of the LA monomer shows a melting and vaporization endotherm at 110 and 117 °C, respectively. These endotherms were absent in the DSC thermogram of the ULMW PLA. In fact, no transitions were observed in the DSC spectrum of the ULMW PLA in the temperature range from ambient to 150 °C, demonstrating that the polymer is a non-crystalline viscous liquid. The DSC thermogram of the PLAF did not show any endotherms (absence of crystalline phase). However, an exothermic transition peakd at 147 °C was observed due to crosslinking of the fumarate groups. It is well established that fumarate groups begin to crosslink in the absence of initiator or crosslinker at tempratures exceeding 140 °C [41]. Based on TGA results, the LA monomer began to evaporate at 110 °C and was competely evapoarted after reaching 185 °C. On the other hand, thermal degradation of the ULMW PLA and PLAF began at 190 and 250 °C, respectively, and was completely degraded after reaching 250 and 370 °C.

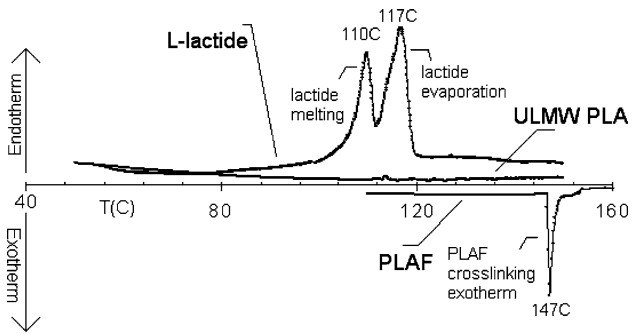

Fig. 5 DSC thermograms of LA, ULMW PLA, and the corresponding PLAF. The PLA was synthesized with LA:DEG ratio of 10

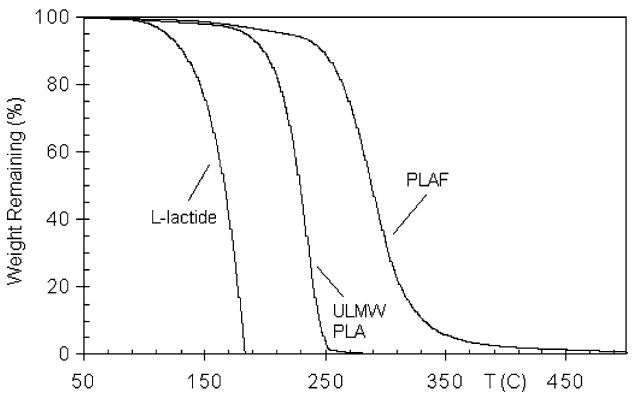

Fig. 6 TGA thermograms of LA, ULMW PLA, and the corresponding PLAF. The PLA was synthesized with LA:DEG ratio of 10

The injectability of the PLAF depended on the amount of NVP crosslinker in the polymerizing mixture. Figure 7 shows the viscosity of the PLAF polymerizing mixtures as a function of shear stress. The visosity of the mixtures was relatively independent of the shear stress. As the amount of NVP relative to PLAF was changed from 30 to 40 and 60% by weight, the mixture viscosity decreased from 70 ± 5 to 7 ± 1 and 2.0 ± 0.5 Pa.S , respetctively, within the range of 1–200 Pa.S for commercially available injectable acrylic bone cements [42].

PLAF is attractive as a reactive macromer in fabrication of bioresorbable injectable in situ crosslinkable scaffolds for tissue regeneration. The PLAF with $\overline{M_n}$ and PDI of 4.1 kDa and 1.5, respectively, was mixed with NVP (30% by weight of PLAF), HA filler, porogen, initiator and accelerator, and the polymerizing mixture was injected into a mold and allowed to crosslink. The porogen was removed and pore morphology was examined with ESEM. The micrographs in Fig. 8 show the cross-section and longitudinal section of the PLAF scaffold. The cross-section shows an interconnected network of pores with average pore size of 300 μm. The PLAF scaffold is degraded in physiologically simulated solutions (PBS or primary culture media) and the rate of degradation depended on the molecular weight of the PLA precursor and the extent of crosslinking (network density) [43]. Osteoconductivity of the scaffold was evaluated in vivo by subcutaneous implantation in nude mice for six weeks. A section of an explanted scaffold is shown in Fig. 9. Significant amount of newly formed woven bone was seen. Blue-purple areas of cartilaginous tissue were also seen indicating a mode of endochondral bone formation.

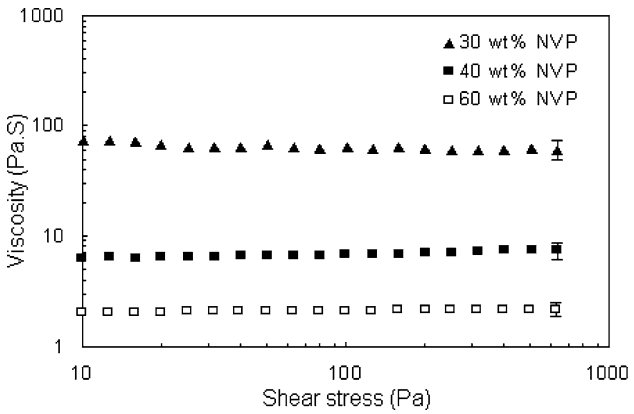

Fig. 7 Viscosity of the PLAF (M_n = 4.1 kDa, PDI = 1.5) polymerizing mixture as a function of shear stress and NVP:PLAF ratio. The PLA was synthesized with LA:DEG ratio of 10

Conclusion

Low molecular weight PLA was synthesized by ring-opening polymerization of L-lactide (LA) using diethylene glycol (DEG) and tin(II) 2-ethylhexanoate as the bifunctional initiator and polymerization catalyst, respectively. After the reaction, the unreacted monomer and DEG were removed under vaccum. Non-solvents methanol, ether, and hexane were used for purification and fractionation of the synthesized polymer. The PLA samples that were precipitated in methanol and ether had a narrow distribution (PDI = 1.2) and resulted in a powder with $\overline{M_n}$ of 4.8 and a wax with $\overline{M_n}$ of 3.6 kDa, respectively. The same PLA sample when precipiated directly in hexane was relatively polydisperse (PDI = 1.6) with $\overline{M_n}$ of 2.3 kDa. The PLA sample in which the supernatant from the ether precipitation was re-precipitated in hexane produced a viscous liquid that had a narrow distribution (PDI = 1.2) with an ultra low $\overline{M_n}$ of 1.2 kDa. Therefore, precipitation of the sythesized PLA in ether followed by re-precipitation of the supernatant in hexane produced an ultra low molecular weight (ULMW) PLA polymer with a narrow distribution. The ULMW PLA was reacted with fumaryl chloride to produce unsaturated in situ crosslinkable poly(lactide fumarate) (PLAF) macromer. Porous scaffolds were produced after injection and in situ crosslinking of the PLAF

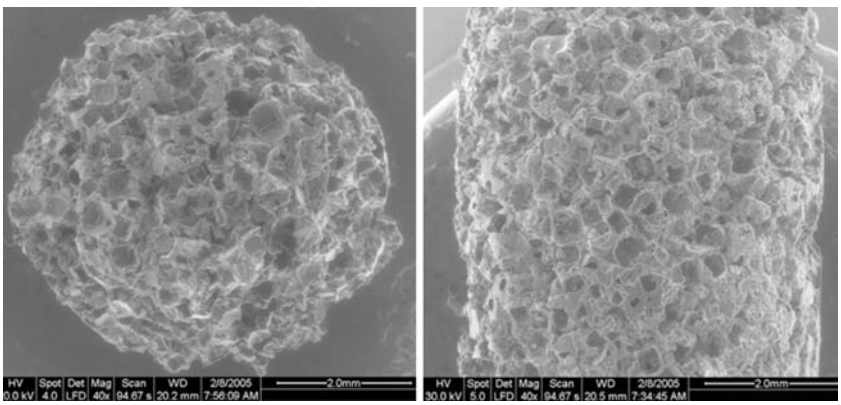

Fig. 8 ESEM micrograph of the cross section (left) and longitudinal section (right) of the porous PLAF scaffold (65% pore volume)

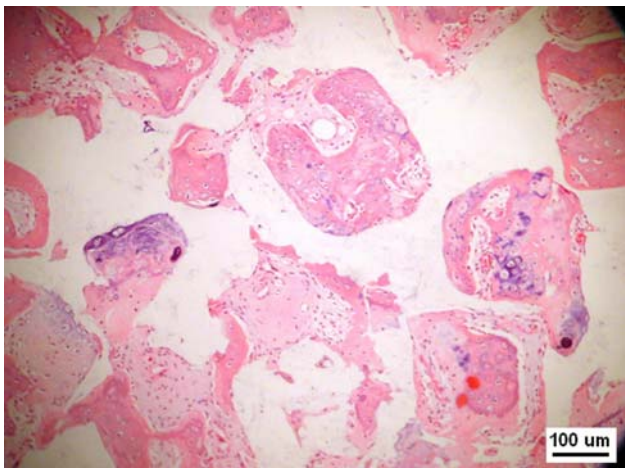

Fig. 9 Histological section of the PLAF scaffold after implantation in nude mice for 6 weeks stained with H&E. The PLAF had $\overline{M_n}$ and PDI of 4.1 kDa and 1.5, respectively. The PLA was synthesized with LA:DEG ratio of 10

macromer with NVP crosslinker in the presence of a porogen. Significant amounts of woven bone was formed when the PLAF scaffold was implanted in nude mice which demonstrated that the scaffold was osteoconductive.

Acknowledgements This work was supported by the Arbeitsgemeinschaft Fur Osteosynthesefragen (AO) Foundation and the Aircast Foundation. The authors like to thank Dr. Alireza Sarvestani for shear viscosity measurements.

References

1. C.-C. CHEN, J.-Y. CHUEH, H. TSENG, H.-M. HUANG and S.-Y. LEE, *Biomaterials* **24** (2003) 1167
2. Y. CHARBIT, C. HITZIG, M. BOLLA, C. BITTON and M. F. BERTRAND, *Biomed. Instrum. Technol*. **33** (1999) 71
3. Surgi-Wrap MAST Bioresorbable Sheet (MAST Biosurgery, San Diego, CA, 2006)
4. S. S. D'SOUZA and P. P. DELUCA, *AAPS Pharm. Sci. Technol*. **6**(2) (2005) E323
5. C. M. PERRY, *Am. J. Clin. Dermatol*. **5**(5) (2004) 361
6. S. K. AGRAWAL, N. SANABRIA-DELONG, J. M. COBURN, G. N. TEW and S. R. BHATIA, *J. Control. Release*. **112**(1) (2006) 64
7. K. UEKI, K. NAKAGAWA, K. MARUKAWA, D. TAKAZAKURA, M. SHIMADA, S. TAKATSUKA and E. YAMAMOTO, *Int. J. Oral. Maxillofac. Surg*. **34**(6) (2005) 627
8. D. B. THORDARSON and G. HURVITZ, *Foot Ankle Int*. **23**(11) (2002) 1003
9. L. WU and J. DING, *J. Biomed. Mater. Res. A*. **75**(4) (2005) 767
10. Y. ZHU, K. S. CHIAN, M. B. CHAN-PARK, P. S. MHAISALKAR and B. D. RATNER, *Biomaterials* **27**(1) (2006) 68
11. R. M. DAY, A. R. BOCCACCINI, V. MAQUET, S. SHUREY, A. FORBES, S. M. GABE, and R. JEROME, *J. Mater. Sci. Mater. Med*. **15**(6) (2004) 729
12. S. W. KANG, O. JEON and B. S. KIM, *Tissue Eng*. **11** (2005) 438
13. E. JABBARI, L. LU and M. J. YASZEMSKI, in "Handbook of Biodegradable Polymeric Materials and Their Applications" (American Scientific Publishers, Stevenson Ranch, CA, 2004) V.2
14. S. S. KIM, M. SUN PARK, O. JEON, C. YONG CHOI and B. S. KIM, *Biomaterials* **27**(8) (2006) 1399
15. J. M. KARP, M. S. SHOICHET and J. E. DAVIES, *J. Biomed. Mater. Res. A*. **64**(2) (2003) 388
16. O. N. MILLER and G. BAZZANO, *Ann. N. Y. Acad. Sci*. **119**(3) (1965) 957
17. H. TSUJI, *Macromol. Biosci*. **5** (2005) 569
18. K. CAI, K. YAO, Y. CUI, Z. YANG, X. LI, H. XIE, T. QING and L. GAO, *Biomaterials* **23**(7) (2002) 1603
19. E. JABBARI, K. W. LEE, A. C. ELLISON, M. J. MOORE, J. A. TESK and M. J. YASZEMSKI, *Trans. Soc. Biomater.* (2004) 1348
20. J. M. TABOAS, R. D. MADDOX, P. H. KREBSBACH and S. J. HOLLISTER, *Biomaterials* **24**(1) (2003) 181
21. E. JABBARI, S. WANG, L. LU, J. A. GRUETZMACHER, S. AMEENUDDIN, T. E. HEFFERAN, B. L. CURRIER, A. J. WINDEBANK and M. J. YASZEMSKI, *Biomacromolecules* **6**(5) (2005) 2503
22. E. JABBARI, L. LU, B.L. CURRIER, A.G. MIKOS and M.J. YASZEMSKI, in "Musculoskeletal Clinical Practice" (American Academy of Orthopaedic Surgeons, Rosemont, IL, 2004) Chap. 32
23. J. S. YOUNG, K. D. GONZALES and K. S. ANSETH, *Biomaterials* **21** (2000) 1181
24. S. J. PETER, P. KIM, A. W. YASKO, M. J. YASZEMSKI and A. G. MIKOS, *J. Biomed. Mater. Res*. **44**(3) (1999) 314
25. J. ZHANG, B. A. DOLL, E. J. BECKMAN and J. O. HOLLINGER, *J. Biomed. Mater. Res. A*. **67**(2) (2003) 389
26. E. JABBARI, A. V. FLORSCHUTZ, L. G. PETERSEN, N. LIU, L. LU, B. L. CURRIER, M. J. YASZEMSKI, *Trans. Soc. Biomaterials* (2004) 512
27. U. BILATI, E. ALLEMANN and E. DOELKER, *J. Microencapsul*. **22**(2) (2005) 205
28. N. A. WEIR, F. J. BUCHANAN, J. F. ORR, D. F. FARRAR and A. BOYD, *Biomaterials* **25**(18) (2004) 3939
29. E. JABBARI, J. A. GRUETZMACHER, L. LU, B. L. CURRIER and M. J. YASZEMSKI, Trans. IEEE Med. Biol. (2003) 1219
30. O. DECHY-CABARET, B. MARTIN-VACA and D. BOURISSOU, *Chem. Rev.* **104**(12) (2004) 6147
31. P. VANDEWITTE, A. BOORSMA, H. ESSELBRUGGE, P. J. DIJKSTRA, J. W. A. VANDENBERG and J. FEIJEN, *Macromolecules* **29**(1) (1996) 212
32. A. TAKASU, Y. IIO, Y. OISHI, Y. NARUKAWA and T. HIRABAYASHI, *Macromolecules* **38** (2005) 1048
33. Z. Y. ZHONG, P. J. DIJKSTRA and J. FEIJEN, *Angewandte Chemie Int. Ed*. **41**(23) (2002) 4510
34. M. BERO, P. DOBRZYNSKI and J. KASPERCZYK, *J. Polym. Sci.: Polym. Chem*. **A37**(22) (1999) 4038
35. E. JABBARI, *J. Microencapsulation* **21**(5) (2004) 525
36. E. JABBARI, J. A. GRUETZMACHER, L. LU, B. L. CURRIER, M. J. YASZEMSKI, *Trans. Soc. Biomaterials* 986 (2004)
37. E. JABBARI and N. A. PEPPAS, *J. Mater. Sci*. **29** (1994) 3969
38. E. JABBARI, Q. K. KANG and Y. H. AN, *MUSC Orthopaedic J*. **8** (2005) 47
39. See http://www.jtbaker.com/msds/O8764.htm for vapor pressure data and http://www.chemrest.com/Toxicity/DiethyleneGlycol.htm for toxicity data of DEG
40. R. M. SILVERSTEIN, G. C. BASSLER and T. C. MORRILL, in "Spectrometric identification of organic compounds" (John Wiley, New York, NY, 1991) 91
41. A. K. SHUNG, M. D. TIMMER, S. B. JO, P. S. ENGEL and A. G. MIKOS, *J. Biomater. Sci. Polym. Ed*. **13**(1) (2002) 95
42. S. J. SULLIVAN and L. D. TOPOLESKI, *J. Biomed. Mater. Res. B Appl. Biomater*. **21** (2006) ahead of print (PubMed #16924654)
43. E. JABBARI, *Trans. Soc. Biomaterials* 491 (2006)